

## Effects of postmetallization annealing on ultrathin SiO<sub>2</sub> layer properties

Asuha, Toshiro Yuasa, Osamu Maida, and Hikaru Kobayashi

Citation: *Applied Physics Letters* **80**, 4175 (2002); doi: 10.1063/1.1482147

View online: <http://dx.doi.org/10.1063/1.1482147>

View Table of Contents: <http://scitation.aip.org/content/aip/journal/apl/80/22?ver=pdfcov>

Published by the [AIP Publishing](#)

---

### Articles you may be interested in

[Nitric acid oxidation of Si method at 120 ° C : HNO<sub>3</sub> concentration dependence](#)

*J. Appl. Phys.* **107**, 054503 (2010); 10.1063/1.3296395

[Ultrathin SiO<sub>2</sub> layer with an extremely low leakage current density formed in high concentration nitric acid](#)

*J. Appl. Phys.* **105**, 103709 (2009); 10.1063/1.3130596

[Modulation of TiSiN effective work function using high-pressure postmetallization annealing in dilute oxygen ambient](#)

*Appl. Phys. Lett.* **92**, 263505 (2008); 10.1063/1.2953192

[Nitric acid oxidation of silicon at 120 ° C to form 3.5-nm SiO<sub>2</sub>/Si structure with good electrical characteristics](#)

*Appl. Phys. Lett.* **85**, 3783 (2004); 10.1063/1.1804255

[Improvement in electrical insulating properties of 10-nm-thick Al<sub>2</sub>O<sub>3</sub> film grown on Al/TiN/Si substrate by remote plasma annealing at low temperatures](#)

*Appl. Phys. Lett.* **80**, 2734 (2002); 10.1063/1.1468916

---



## Effects of postmetallization annealing on ultrathin SiO<sub>2</sub> layer properties

Asuha, Toshiro Yuasa, Osamu Maida, and Hikaru Kobayashi<sup>a)</sup>

*Institute of Scientific and Industrial Research, Osaka University and CREST, Japan Science and Technology Corporation, 8-1, Mihogaoka, Ibaraki, Osaka 567-0047, Japan*

(Received 27 December 2001; accepted for publication 3 April 2002)

Observation of both longitudinal optical and transverse optical phonons of  $\sim 1.3$  nm ultrathin silicon dioxide (SiO<sub>2</sub>) layers formed by immersion in nitric acid shows that the SiO<sub>2</sub> density increases by 16% after postoxidation annealing (POA) at 900 °C. For the SiO<sub>2</sub> layers without POA, postmetallization annealing (PMA) greatly decreases the SiO<sub>2</sub> thickness from 1.3 to 0.2 nm, the effect of which is attributable to the reaction of aluminum with SiO<sub>2</sub> to form a metallic mixture of aluminum oxide and Si. For SiO<sub>2</sub> layers with POA, PMA decreases the SiO<sub>2</sub> thickness to a lesser extent (from 1.4 to 0.9 nm), because of the suppression of aluminum diffusion into SiO<sub>2</sub> due to its dense structure. PMA is found to decrease the interface state density but increase the leakage current density. © 2002 American Institute of Physics. [DOI: 10.1063/1.1482147]

For fabrication of metal–oxide–semiconductor (MOS) devices, low-temperature postmetallization annealing (PMA) of gate oxide layers is a very important procedure in order to passivate interface states.<sup>1</sup> Aluminum (Al) is often used as an electrode material for PMA.<sup>1–4</sup> According to the model proposed by Deal, Mackenna, and Castro,<sup>5</sup> atomic hydrogen is formed by the reaction of water present in silicon dioxide (SiO<sub>2</sub>) layers with active metals such as Al and magnesium, followed by its diffusion to the interface, and then reacts with interface states, resulting in their passivation. It is reported that for a decrease in the interface state density, PMA is more effective than postoxidation annealing (POA),<sup>2,3</sup> and it has been concluded that there exist interface states that can be eliminated by atomic hydrogen but not by molecular hydrogen.<sup>2</sup> In the above studies, SiO<sub>2</sub> layers thicker than 2 nm were employed, without investigating ultrathin SiO<sub>2</sub> layers, which would be important for future ultra-large-scale integration.

In the present work, we investigate the effects of PMA on the chemical structure and electrical characteristics of chemically grown SiO<sub>2</sub> layers with the 1.3–1.4 nm thickness.

Phosphorus-doped *n*-type Si(100) wafers with a  $\sim 10$   $\Omega$  cm resistivity were cleaned using the RCA method and etched with a 5% hydrofluoric acid solution. Next, ultrathin chemical SiO<sub>2</sub> layers were formed by immersion of the wafers in a concentrated nitric acid (HNO<sub>3</sub>) solution at 113 °C. POA was performed at 900 °C in nitrogen for 15 min, and then Al dots ( $\sim 200$  nm) with a 0.15 mm diam were formed on the SiO<sub>2</sub> layers, resulting in an  $\langle \text{Al}/\text{ultrathin SiO}_2/\text{Si}(100) \rangle$  MOS structure. Then, PMA was carried out at 400 °C in 5% H<sub>2</sub>+95% N<sub>2</sub> for 10 min. This PMA temperature has been reported to reduce the interface state density of thermally grown SiO<sub>2</sub>/Si to the lowest value.<sup>1</sup>

Fourier transformed infrared (FTIR) transmission spectra were recorded using a Nicolet Nexus 370S spectrometer in a dry-nitrogen atmosphere with the energy resolution and incident angle set at 4 cm<sup>-1</sup> and 65°, respectively. Measure-

ments of x-ray photoelectron spectroscopy (XPS) spectra were performed using a VG Scientific ESCALAB 220i-XL spectrometer with a monochromatic Al *K* $\alpha$  radiation source. Photoelectrons were detected at the surface-normal direction. Capacitance–voltage (*C–V*) measurements were performed with an HP 4192A LF impedance analyzer at 100 k and 1 MHz.

Figure 1 shows the FTIR spectra in the Si–O asymmetric stretching vibrational region for the ultrathin SiO<sub>2</sub>/Si(100) structure formed in HNO<sub>3</sub>. For the SiO<sub>2</sub> layers without POA, absorption peaks due to longitudinal optical (LO) and transverse optical (TO) phonons were observed at 1219 and 1049 cm<sup>-1</sup>, respectively. POA at 900 °C greatly shifted the LO peak to 1247 cm<sup>-1</sup> while the TO peak was only slightly shifted to 1053 cm<sup>-1</sup>.

Queoney *et al.*<sup>6</sup> have shown, using the effective medium approximation, that inclusion of foreign species (i.e., pores, SiO, or Si) in SiO<sub>2</sub> with 20% concentration nominally shifts the LO and TO peaks. In the presence of larger concentrations of pores, the LO and TO peaks are shifted toward the lower and higher energies, respectively. These results of the calculations are in disagreement with the present experimental results. Therefore, although POA probably eliminates a low concentration of pores, this is not the main reason for the

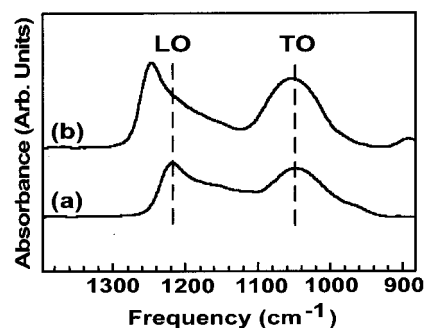


FIG. 1. FTIR spectra in the asymmetric Si–O stretching vibrational region for the ultrathin chemical SiO<sub>2</sub>/Si structure: (a) without POA and (b) with POA at 900 °C.

<sup>a)</sup>Electronic mail: h.kobayashi@sanken.osaka-u.ac.jp

large shift of the LO peak. Since shifts caused by foreign species in SiO<sub>2</sub> are negligibly small, the SiO<sub>2</sub> layer can be regarded as a homogeneous medium. In this case, using the central and noncentral force approximation, the vibrational frequencies of TO and LO phonons,  $\nu_{\text{TO}}$  and  $\nu_{\text{LO}}$ , are given by<sup>7</sup>

$$\nu_{\text{TO}} = \frac{1}{2\pi} \sqrt{2[\alpha \sin^2(\theta/2) + \beta \cos^2(\theta/2)]/m}, \quad (1)$$

$$\nu_{\text{LO}} = \frac{1}{2\pi} \sqrt{2[\alpha \sin^2(\theta/2) + \beta \cos^2(\theta/2) + Z^2 \rho / \epsilon_{\infty} (2m + M)]/m}, \quad (2)$$

where  $\alpha$  and  $\beta$  are the central and noncentral force constants, respectively,  $\theta$  is the Si–O–Si bridging bond angle,  $m$  and  $M$  are the atomic masses of oxygen and Si atoms, respectively,  $\epsilon_{\infty}$  is the permittivity at the infinite frequency,  $Z$  is the electrical charge related to the movement of oxygen atoms, and  $\rho$  is the atomic density of SiO<sub>2</sub>. Only the slight increase in  $\nu_{\text{TO}}$  by POA shows that the bond angle,  $\theta$ , is not largely altered. On the other hand,  $\nu_{\text{LO}}$  is greatly increased by POA, and this increase is most probably attributable to an increase in the atomic density of SiO<sub>2</sub>,  $\rho$ , by  $\sim 16\%$ . This increase in  $\rho$  may result from a change in the SiO<sub>2</sub> network structure with atomic order size pores to that without it.

From Eqs. (1) and (2) we have

$$\nu_{\text{LO}}^2 - \nu_{\text{TO}}^2 = C\rho, \quad (3)$$

where  $C$  is a constant. Using the values for thick SiO<sub>2</sub> layers, i.e.,  $\nu_{\text{TO}}$  of 1090 cm<sup>-1</sup>,  $\nu_{\text{LO}}$  of 1256 cm<sup>-1</sup>, and  $\rho$  of  $2.28 \times 10^{22}$  cm<sup>-3</sup>,<sup>8</sup>  $\rho$  for the chemical SiO<sub>2</sub> layers without and with POA is estimated to be  $2.20 \times 10^{22}$  and  $2.55 \times 10^{22}$  cm<sup>-3</sup>, respectively. It is calculated that the geometrical effect slightly increases  $\nu_{\text{TO}}$  with the oxide thickness,  $d_{\text{ox}}$  (i.e., 2 cm<sup>-1</sup> between  $d_{\text{ox}} = 2$  nm and  $d_{\text{ox}} = 40$  nm) while  $\nu_{\text{LO}}$  is independent of  $d_{\text{ox}}$ .<sup>8</sup> In the estimation of  $\rho$ , the shift in  $\nu_{\text{TO}}$  caused by the geometrical effect is assumed to be 5 cm<sup>-1</sup> between the  $\sim 1.4$  nm SiO<sub>2</sub> layers employed in the present study and bulk SiO<sub>2</sub>, whose  $\nu_{\text{LO}}$ ,  $\nu_{\text{TO}}$ , and  $\rho$  values are used for the calculation of  $C$  in Eq. (3).

Olsen and Shimura<sup>9</sup> and Boyd and Wilson<sup>10</sup> have observed that the vibrational frequency of TO phonons for thermal SiO<sub>2</sub> layers decreases as the SiO<sub>2</sub> thickness becomes thinner, and attributed the shift to the strain near the interface. In other studies, it is observed that both the vibrational frequencies of LO and TO phonons increase with the SiO<sub>2</sub> thickness or the oxidation temperature, the result of which requires complicated analysis, resulting in the various attributions of the shifts, i.e., stoichiometry changes,<sup>11</sup> inhomogeneity,<sup>6</sup> and roughness near the interface.<sup>12</sup> It should be noted that in the present study,  $\nu_{\text{LO}}$  increases after POA while  $\nu_{\text{TO}}$  is almost unchanged, leading to the clearer conclusion of the densification of the SiO<sub>2</sub> layer by POA.

Figure 2 shows the XPS spectra in the Si 2*p* region for the ultrathin chemical SiO<sub>2</sub>/Si(100) structure. For spectra (a), POA was not performed before the Al deposition, while for spectra (b), it was carried out at 900 °C in nitrogen for 15 min. The upper spectra were observed before the Al deposition. For the lower spectra, on the other hand, the Al depo-

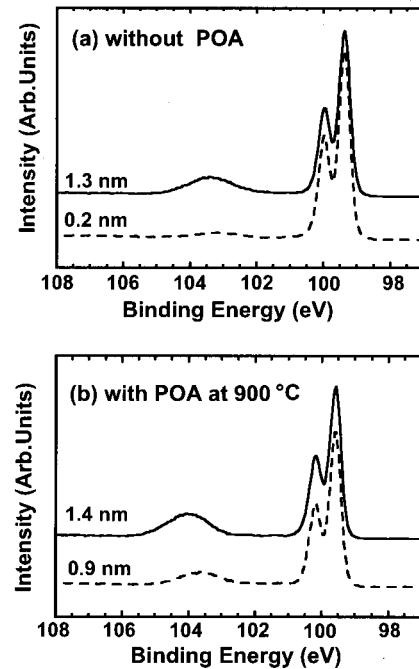


FIG. 2. XPS spectra in the Si 2*p* region for the ultrathin chemical SiO<sub>2</sub>/Si structure: (a) without POA and (b) with POA at 900 °C. Solid and dashed lines are for the SiO<sub>2</sub> layers without and with PMA at 400 °C, respectively.

sition and PMA were performed and the Al layer was etched away using a HCl:H<sub>2</sub>O = 1:3 solution just before the XPS measurements. The SiO<sub>2</sub> thickness was estimated from the area intensity ratio between the oxide and substrate Si 2*p* peaks using 3.2 and 2.7 nm as the mean-free paths of photoelectrons in the SiO<sub>2</sub> layer and the Si substrate, respectively.

For the SiO<sub>2</sub> layers without POA [spectra (a)], the intensity of the oxide Si 2*p* peak was markedly decreased by PMA, and the SiO<sub>2</sub> thicknesses before and after PMA were estimated to be 1.3 and 0.2 nm, respectively. For the SiO<sub>2</sub> layers with POA [spectra (b)], PMA decreases the SiO<sub>2</sub> thickness only slightly from 1.4 to 0.9 nm. The experimental results show that Al reduces SiO<sub>2</sub> with the following reaction formula:



This reaction has a negative Gibbs free-energy change ( $\Delta G = -581.9$  kJ mol<sup>-1</sup>), and thus it proceeds spontaneously. In the previous study, in fact, the formation of Al<sub>2</sub>O<sub>3</sub> and Si was observed after PMA by means of XPS.<sup>13</sup> It was also observed that at high temperatures (e.g., 510 °C) Al reacts with thick SiO<sub>2</sub>, resulting in the formation of thick (e.g.,  $\sim 200$  nm) Al<sub>2</sub>O<sub>3</sub> and Si.<sup>14</sup> XPS measurements in the present study, however, show that Al<sub>2</sub>O<sub>3</sub> is not present on Si after the etch off of the Al layer because it is soluble in HCl.

The different magnitudes of the decrease in the thickness of the SiO<sub>2</sub> layers without and with POA are attributable to the variation in the SiO<sub>2</sub> density. FTIR measurements show that the atomic density increases by  $\sim 16\%$  after POA at 900 °C, as described above. It is likely that Al readily diffuses into the SiO<sub>2</sub> layers when the layers are less dense and then reacts with SiO<sub>2</sub>. On the other hand, the SiO<sub>2</sub> layers with POA have a dense structure, resulting in the suppression

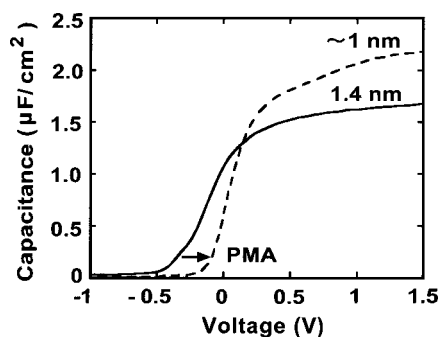


FIG. 3.  $C$ - $V$  curves for  $\langle\text{Al}/\text{ultrathin chemical SiO}_2/\text{Si}(100)\rangle$  MOS diodes in which POA was performed at 900 °C. Solid and the dashed lines are for the diodes without and with PMA at 400 °C, respectively.

of the Al diffusion. Consequently, only the surface region of the  $\text{SiO}_2$  layers is transformed to  $\text{Al}_2\text{O}_3$  and Si by PMA.

Figure 3 shows the  $C$ - $V$  curves for the  $\langle\text{Al}/\text{ultrathin SiO}_2/n\text{-Si}(100)\rangle$  MOS structure. In order to eliminate the effect of a leakage current on the capacitance measurements, we have adopted the two-frequency method.<sup>15</sup> PMA causes a shrinkage of the bias region in which the capacitance changes greatly. This shrinkage is attributable to a decrease in the interface state density, the result of which is consistent with those obtained for thermal  $\text{SiO}_2$  layers.<sup>1-5</sup> It is highly probable that a trace amount of water is present in  $\text{SiO}_2$  even after POA.<sup>1</sup> Water reacts with Al to form atomic hydrogen (H):



The atomic hydrogen produced migrates to the Si/SiO<sub>2</sub> interface, and then reacts with interface states to make them electrically inactive.<sup>5</sup> For this reason, the  $C$ - $V$  curve becomes steeper after PMA.

Another change caused by PMA is an increase in the saturation capacitance. This increase is attributable to a reduction in the  $\text{SiO}_2$  thickness, as is evident from the XPS result shown in Fig. 2. If we adopt 3.9 (i.e.,  $\text{SiO}_2$  bulk dielectric constant) as the relative dielectric constant of the ultrathin  $\text{SiO}_2$  layers, the effective  $\text{SiO}_2$  thicknesses without and with PMA were estimated to be 2.0 and 1.6 nm, respectively, from the saturation capacitances. These values are much larger than those estimated from XPS spectra. Such a discrepancy is often reported<sup>15,16</sup> and may result from the different electronic structure from that of bulk  $\text{SiO}_2$ , leading to a lower dielectric constant.

The flatband voltages for the  $C$ - $V$  curves in Fig. 3 of nearly zero differ from that predicted from the difference in the work function between  $n$ -Si and Al (i.e.,  $-0.3$  V). This shift possibly results from an increase in the effective work

function of the Al layer by oxygen adsorption and/or oxide fixed negative charges in the order of  $10^{11}$   $\text{cm}^{-2}$ .

The density of the leakage current was markedly increased by PMA for the MOS diodes even with POA, (i.e., from 0.4 to 6  $\text{A cm}^{-2}$  at the gate bias,  $V_G$ , of 1.5 V). This increase is attributable to the decrease in the  $\text{SiO}_2$  thickness, and indicates that the layer formed by PMA consists of a mixture of  $\text{Al}_2\text{O}_3$  and Si and that the mixture has a metallic character.

It is well known that Si penetrates into Al layers through the weak points of  $\text{SiO}_2$  layers, leading to an increase in the leakage current.<sup>17,18</sup> In the case of such a spiking effect, deep pits were observed in the scanning electron microscopy micrographs after the removal of the Al layers.<sup>18</sup> In the present experiments, no pits were observed in the secondary electron micrographs, indicating that the increase in the leakage current density was not due to the spiking effect but the reaction between Al and  $\text{SiO}_2$ .

In conclusion, although PMA passivates interface states, the density of the leakage current for the ultrathin  $\text{SiO}_2$  layers increases. This increase results from a decrease in the  $\text{SiO}_2$  thickness caused by the reaction of Al with  $\text{SiO}_2$ . The magnitude of the decrease in thickness strongly depends on whether POA is performed or not. This dependence is attributable to the variation in the  $\text{SiO}_2$  density, which in turn affects the magnitude of the Al diffusion into  $\text{SiO}_2$ .

<sup>1</sup>E. H. Nicollian and J. R. Brews, *MOS (Metal Oxide Semiconductor) Physics and Technology* (Wiley, New York, 1982), Chap. 15.

<sup>2</sup>J. F. Zhang, P. Watkinson, S. Taylor, and W. Eccleston, *Appl. Surf. Sci.* **39**, 374 (1989).

<sup>3</sup>M. Depas, R. L. Van Meirhaeghe, W. H. Lafière, and F. Cardon, *Solid-State Electron.* **37**, 433 (1994).

<sup>4</sup>D. R. Young, *J. Appl. Phys.* **52**, 4090 (1981).

<sup>5</sup>B. E. Deal, E. L. Mackenna, and P. L. Castro, *J. Electrochem. Soc.* **116**, 997 (1969).

<sup>6</sup>K. T. Queeney, M. K. Weldon, J. P. Chang, Y. J. Chabal, A. B. Gurevich, J. Sapjeta, and R. L. Opila, *J. Appl. Phys.* **87**, 1322 (2000).

<sup>7</sup>A. Lehman, L. Schuman, and K. Hübner, *Phys. Status Solidi B* **117**, 689 (1983).

<sup>8</sup>C. Martinet and R. A. B. Devine, *J. Appl. Phys.* **77**, 4343 (1995).

<sup>9</sup>J. E. Olsen and F. Shimura, *Appl. Phys. Lett.* **53**, 1934 (1988).

<sup>10</sup>I. W. Boyd and J. I. B. Wilson, *J. Appl. Phys.* **62**, 3195 (1987).

<sup>11</sup>R. A. B. Devine, *Appl. Phys. Lett.* **68**, 3108 (1996).

<sup>12</sup>K. Ishikawa, H. Ogawa, and S. Fujimura, *J. Appl. Phys.* **85**, 4076 (1999).

<sup>13</sup>M. H. Hecht, R. P. Vasquez, F. J. Grunthaner, N. Zamani, and J. Maserjian, *J. Appl. Phys.* **57**, 5256 (1985).

<sup>14</sup>R. J. Blattner and A. J. Braundmeier, Jr., *J. Vac. Sci. Technol.* **20**, 320 (1982).

<sup>15</sup>K. J. Yang and C. Hu, *IEEE Trans. Electron Devices* **46**, 1500 (1999).

<sup>16</sup>G. Timp *et al.*, *Microelectron. Reliab.* **40**, 557 (2000).

<sup>17</sup>M.-J. Jeng, H.-S. Lin, and J.-G. Hwu, *Jpn. J. Appl. Phys., Part 1* **34**, 6008 (1995).

<sup>18</sup>L. S. Hung, J. W. Mayer, M. Zhang, and E. D. Wolf, *Appl. Phys. Lett.* **43**, 1123 (1983).